INDIRECT GEOREFERENCING OF AIRBORNE MULTI-LINE ARRAY SENSORS: A SIMULATED CASE STUDY

Daniela Poli

Institute of Geodesy and Photogrammetry
Swiss Federal Institute of Technology, Zurich, Switzerland
daniela@geod.baug.ethz.ch

KEY WORDS: Orientation, Modelling, Triangulation, GPS/INS, Three Line, Simulation

ABSTRACT:

Multi-line array sensors, carried on airborne or satellite, acquire images with along or across track stereo viewing and are used for photogrammetric mapping at different scales. The main characteristic of the imagery provided by this kind of sensors is that each image line is independently acquired with a different sensor external orientation (position, attitude). If positioning instruments (GPS/INS) carried on board provide the sensor external orientation of each line, the ground coordinates of the observed points can be estimated with direct georeferencing. Anyway the positional and angular displacements of the GPS/INS instruments with respect to the image frame with origin in the sensor perspective centre must be estimated, together with additional measurement errors contained in the observations. Therefore a triangulation integrated with the sensor external orientation modelling (indirect georeferencing) has been implemented. The algorithms have been tested on a simulated testfield, supposing an airborne three-line sensor with optical system consisting of one lens. After simulating the sensor trajectory and the coordinates of 40 object points, the image coordinates of each point in the three images were calculated with back projection. In order to test the indirect georeferencing model, some perturbations and constant offsets in the correct sensor external orientation were introduced and afterwards estimated with the proposed integrated triangulation. The RMS obtained on the checkpoints using different Ground Control Points (GCPs) and Tie Points (TPs) distributions are presented.

1. INTRODUCTION

Today a wide class of linear CCD array sensors that acquire images in a pushbroom mode exists. Some of them are carried on aircraft (e.g. ADS40, DPA and WAAC from DLR, AirMISR from NASA) or helicopter (e.g. TLS from STARLABO), others on spacecraft (e.g. SPOT from CNES, IRS from ISRO, MISR and ASTER from NASA, IKONOS from SpaceImage, WAOSS from DLR) and can be used for photogrammetric mapping at different resolutions.

The stereoscopy of the images is achieved across- or along-track with respect to the flight direction. Sensors with across-track stereo capability, usually carried on spacecraft (SPOT, IRS), combine one linear CCD array with a rotating mirror. Stereopairs are acquired from different orbits, with a time delay in the order of days or months. On the other hand, sensors with along-track stereo capability scan the terrain surface with linear CCD arrays placed parallel to each other and with different viewing angles along the flight direction. The advantage of this geometry is to enable the acquisition of a larger number of images with a small time delay. A very common along-track stereo system used both on airborne (ADS40, TLS, DPA, WAAC) and satellite (MOMS-02, WAOSS) consists of three CCD lines looking forward, nadir and backward the flight direction. Within pushbroom sensors with along-track stereo viewing, the number of lenses is variable: some sensors (ADS40, TLS, DPA, WAAC, WAOSS) use one lens common for all the CCD arrays, others (AirMISR, MISR) have one lens for each group of CCD lines looking in the same direction.

The images provided by linear CCD array sensors consist of lines independently acquired with a different exterior orientation. Therefore a classic bundle adjustment is not realistic for the georeferencing of this kind of imagery, because the number of unknowns would be huge.

In case of sensors carried on satellite, due to the smooth trajectory, the exterior orientation can be modelled as a polynomial function depending on time, including the physical properties of the satellite orbit as constraints (Kratky, 1989; Ebner, 1992,). In this case a sufficient number of well-distributed Ground Control Points (GCPs) is required.

For airborne applications, where the trajectory is not predictable, the direct measurement of the external orientation is indispensable. Thanks to the successful improvement and rapid expanding of positioning systems, the exterior orientation can be directly measured with high precision with GPS and INS systems carried on board (Cramer et al., 2000), allowing direct georeferencing and rectification of the images (Schwarz, 1996; Haala et al., 1998, Tempelmann et al., 2000).

Anyway the data provided by GPS/INS do not refer to the perspective centre of the lens, but to additional reference systems centred in the instruments themselves. The required offset vectors and misalignment angles between the systems are measured before the flight with surveying methods. Anyway these data are not always available and must be estimated with post-flight calibration procedures. Moreover the GPS/INS observations can be affected by additional errors. Therefore for high precision applications the errors contained in the GPS/INS data have to be modelled and integrated in the bundle adjustment of the imagery, resulting in an indirect georeferencing (Lee et al., 2000; Chen, 2001).

In this paper a model for indirect georeferencing of multi-line CCD array sensors is proposed. After an overview on direct georeferencing of multi-line sensors (Section 2), the proposed model for indirect georeferencing is presented in Sections 3. Then, after the description of the generation of a simulated testfield for an airborne three-line sensor (Section 4), the results obtained from the indirect georeferencing are presented and discussed in Section 5. Conclusions and future work about the extension of the model to multi-lens linear CCD array sensors will close the paper.

2. GEOREFERENCING OF MULTI-LINE SENSORS IMAGERY

The aim of georeferencing is to establish a relationship between image and ground reference systems, according to the sensor geometry and the available data. The image system is centred in the lens perspective centre (PC), with *x*-axis tangent to the flight trajectory, *z*-axis parallel to the optical axis and pointing upwards and *y*-axis along the CCD line, completing a right-hand coordinate system (Figure 1).

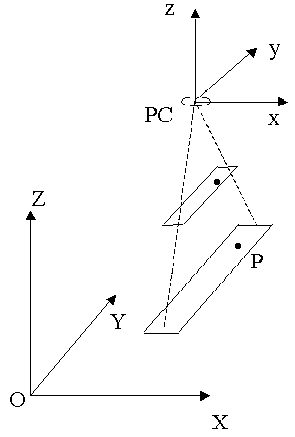

Figure 1. Image and ground reference systems.

In case of CCD linear array scanners with along-track stereo capability, each image line is the result of a nearly parallel projection in the flight direction and a perspective projection in the CCD line direction. The relationship between image and ground coordinates of each observed point is described by:

$$\begin{bmatrix} X \\ Y \\ Z \end{bmatrix} = \begin{bmatrix} X_C \\ Y_C \\ Z_C \end{bmatrix} + kR^T(\omega_C, \varphi_C, \kappa_C) \begin{bmatrix} x \\ y \\ -f \end{bmatrix} \quad (1)$$

where:

$[X\ Y\ Z]$: point coordinates in the ground system;
$[X_C\ Y_C\ Z_C]$: PC position in the ground system;
$[x\ y\ -f]$: point coordinates in the image system;
f: focal length;
k: scale factor;
$R(\omega_C, \varphi_C, \kappa_C)$: rotation matrix from image to ground system, according to attitude angles $\omega_C, \varphi_C, \kappa_C$.

Solving Equation 1 with respect to *x* and *y*, the collinearity equations:

$$\begin{aligned} x &= -f \cdot \frac{r_{11}(X-X_C) + r_{21}(Y-Y_C) + r_{31}(Z-Z_C)}{r_{13}(X-X_C) + r_{23}(Y-Y_C) + r_{33}(Z-Z_C)} \\ y &= -f \cdot \frac{r_{12}(X-X_C) + r_{22}(Y-Y_C) + r_{32}(Z-Z_C)}{r_{13}(X-X_C) + r_{23}(Y-Y_C) + r_{33}(Z-Z_C)} \end{aligned} \quad (2)$$

are obtained.
For sensors whose optical systems consist of more lenses, additional geometric parameters describing the relative position and attitude of each lens with respect to the nadir one are imported in the collinearity model (Ebner, 1992). Calling f_j the focal length, Δx_j, Δy_j, Δz_j the relative position and α_j, β_j, γ_j the relative attitude of each lens *j*, Equation 1 is extended to:

$$\begin{bmatrix} X \\ Y \\ Z \end{bmatrix} = \begin{bmatrix} X_C \\ Y_C \\ Z_C \end{bmatrix} + D(\omega_C, \varphi_C, \kappa_C) \begin{bmatrix} \Delta x_j \\ \Delta y_j \\ \Delta z_j \end{bmatrix} + kR(\omega_C, \varphi_C, \kappa_C, \alpha_j, \beta_j, \gamma_j) \begin{bmatrix} x \\ y \\ -f_j \end{bmatrix} \quad (3)$$

where:

$M(\alpha_j, \beta_j, \gamma_j)$: rotation from image system centred in the off-nadir lens *j* to image system with origin in the central lens;
$D(\omega_C, \varphi_C, \kappa_C)$: rotation from image system centred in the central lens to ground frame.
$R = D(\omega_C, \varphi_C, \kappa_C) M(\alpha_j, \beta_j, \gamma_j)$: complete rotation from image system centred in the off-nadir lens *j* to ground frame.

The collinearity equations obtained from Equation 3 are:

$$\begin{aligned} x &= -f_j \cdot \frac{r_{11}(X-X_C) + r_{21}(Y-Y_C) + r_{31}(Z-Z_C) - (m_{11}\Delta x_j + m_{21}\Delta y_j + m_{31}\Delta z_j)}{r_{13}(X-X_C) + r_{23}(Y-Y_C) + r_{33}(Z-Z_C) - (m_{13}\Delta x_j + m_{23}\Delta y_j + m_{33}\Delta z_j)} \\ y &= -f_j \cdot \frac{r_{12}(X-X_C) + r_{22}(Y-Y_C) + r_{32}(Z-Z_C) - (m_{12}\Delta x_j + m_{22}\Delta y_j + m_{32}\Delta z_j)}{r_{13}(X-X_C) + r_{23}(Y-Y_C) + r_{33}(Z-Z_C) - (m_{13}\Delta x_j + m_{23}\Delta y_j + m_{33}\Delta z_j)} \end{aligned} \quad (4)$$

If the relative orientation parameters are equal to zero (nadir case), Equations 1 and 2 are obtained from Equations 3 and 4.
The algorithms that will be presented have been developed both for one-lens and multi-lens CCD linear sensors.
Assuming that the focal lengths and the additional parameters are known, in order to solve Equation 1 and 3, six external orientation parameters (position, attitude) are required for each exposure. Therefore using Ground Control Points (GCPs) and Tie Points (TPs), a bundle adjustment for the external orientation and ground coordinates estimation is not realistic, because the number of unknown would be too large.
Anyway in most airborne applications, instruments carried on board provide the sensor external orientation of each image line and allow the estimation of the ground coordinates with direct georeferencing.

2.1 Direct georeferencing

In case of sensors carried on aircraft the direct measurement of the external orientation is indispensable, because the trajectory is unpredictable and the effects of the flight turbulence are not negligible. Nowadays GPS/INS instruments carried on board, together with accurate filtering techniques, provide the sensor external orientation of each image line and allow the estimation of the ground coordinates with forward intersection (Poli, 2001). Anyway the observations provided by GPS/INS do not refer to the camera PC: the position data refer to a local system with origin in the GPS antenna and the attitude refer to a local frame centred in the INS instrument (Figure 2). These two systems are shifted and rotated with respect to the image one, therefore the collinearity equations (Equations 1 and 3) have to be extended in order to include the offset vectors and the misalignment angles between the image and the GPS and INS frames (Schwarz, 1996).
The extended collinearity equations for one-lens sensors are:

$$\begin{bmatrix} X \\ Y \\ Z \end{bmatrix} = \begin{bmatrix} X_{GPS} \\ Y_{GPS} \\ Z_{GPS} \end{bmatrix} + R_{INS}^{G} \left(R_{GPS}^{INS} \begin{bmatrix} \Delta X_{GPS} \\ \Delta Y_{GPS} \\ \Delta Z_{GPS} \end{bmatrix} + kR_c^{INS} \begin{bmatrix} x \\ y \\ -f \end{bmatrix} \right) \quad (5)$$

where:

$[X\ Y\ Z]$: point coordinates in the ground system;

$[X_{GPS}\ Y_{GPS}\ Z_{GPS}]$: observed GPS antenna position;

$[\Delta X_{GPS}\ \Delta Y_{GPS}\ \Delta Z_{GPS}]$: offset vector between GPS and image frames;

$[x\ y\ -f]$: point coordinates in the image system;

f: focal length;

$R_c^{INS}(\Delta\omega_c, \Delta\varphi_c, \Delta\kappa_c)$: rotation from the image to INS systems;

$R_{GPS}^{INS}(\Delta\omega_{GPS}, \Delta\varphi_{GPS}, \Delta\kappa_{GPS})$: rotation from the GPS to INS systems;

$R_{INS}^{G}(\omega_{INS}, \varphi_{INS}, \kappa_{c\backslash INS})$: rotation from INS to ground system, using angles observed by INS system;

k: scale factor.

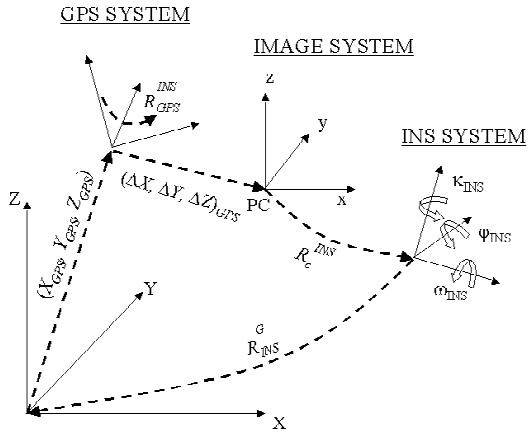

Figure 2. Reference systems in direct georeferencing algorithm.

In the same way, the collinearity equations for multi-lens sensors are extended in order to take into account the GPS/INS misalignments and drifts.

3. INDIRECT GEOREFERENCING

If the misalignments between GPS, INS and image systems are known, the ground coordinates of the points observed in the stereo images can be calculated with forward intersection based on Equation 5. Anyway in most cases the GPS offset and INS drift angles are not available, so the direct georeferencing algorithm can not be applied. The GPS/INS misalignment have to be estimated with post-flight calibration procedures, together with any additional measurements errors that may be contained in the GPS/INS observations. The solution is achieved by including in the standard photogrammetric triangulation suitable functions that model the sensor external orientation and take into account the GPS and INS measurements. The complete procedure is called indirect georeferencing model. The proposed trajectory model is based on piecewise polynomial functions depending on time.

3.1 Trajectory modelling

The aircraft trajectory is divided into segments, according to the number and distribution of GCPs and TPs. For each segment *i*, delimited by the time extremes t_{ini}^{i} and t_{fin}^{i}, the variable:

$$\bar{t} = \frac{t - t_{ini}^{i}}{t_{fin}^{i} - t_{ini}^{i}} \in [0,1] \tag{6}$$

is defined, where t is the acquisition time of the processed line. Then in each segment the sensor attitude and position (X_C, Y_C, Z_C, ω_C, φ_C, κ_C) are modelled with a second order polynomial function depending on $\bar{t}$:

$$\begin{aligned}
X_C(\bar{t}) &= X_{instr} + X_0^i + X_1^i\bar{t} + X_2^i\bar{t}^2 \\
Y_C(\bar{t}) &= Y_{instr} + Y_0^i + Y_1^i\bar{t} + Y_2^i\bar{t}^2 \\
Z_C(\bar{t}) &= Z_{instr} + Z_0^i + Z_1^i\bar{t} + Z_2^i\bar{t}^2 \\
\omega_C(\bar{t}) &= \omega_{instr} + \omega_0^i + \omega_1^i\bar{t} + \omega_2^i\bar{t}^2 \\
\varphi_C(\bar{t}) &= \varphi_{instr} + \varphi_0^i + \varphi_1^i\bar{t} + \varphi_2^i\bar{t}^2 \\
\kappa_C(\bar{t}) &= \kappa_{instr} + \kappa_0^i + \kappa_1^i\bar{t} + \kappa_2^i\bar{t}^2
\end{aligned} \tag{7}$$

where:

$[X_{instr}\ Y_{instr}\ Z_{instr}]$: PC position observed with GPS;

$[\omega_{instr}\ \varphi_{instr}\ \kappa_{instr}]$: PC attitude observed with INS;

$[X_0\ \ldots\ \kappa_2]_i$: 18 unknown parameters modelling the external orientation in segment *i*.

The constant terms describe the shifts and angular drifts between the image system and, respectively, the GPS and INS systems, while the linear and quadratic terms model the additional errors in GPS/INS measurements.

If the time interval between exposure of adjacent image lines is constant, the image line number *l* can be used in place of the time. In this case, calling l_{ini}^{i} and l_{fin}^{i} the first and last lines of segment *i*, $\bar{t}$ is defined as:

$$\bar{t} = \frac{l - l_{ini}^{i}}{l_{fin}^{i} - l_{ini}^{i}} \in [0,1] \tag{8}$$

At the points of conjunction between adjacent segments, constraints on the zero, first and second order continuity are imposed on the trajectory functions: we force that the values of the functions and their first and second derivatives computed in two neighbouring segments are equal at the segments boundaries. As the point on the border between segment *i* and *i+1* has $\bar{t}=1$ in segment *i* and $\bar{t}=0$ in segment *i+1*, imposing the zero order continuity for *X* function, we obtain:

$$X_C^i\Big|_{\bar{t}=1} = X_C^{i+1}\Big|_{\bar{t}=0} \tag{9}$$

It yields to:

$$X_0^i + X_1^i + X_2^i = X_0^{i+1} \tag{10}$$

In the same way, we get:

$$\begin{aligned} Y_0^i+Y_1^i+Y_2^i&=Y_0^{i+1}\\ Z_0^i+Z_1^i+Z_2^i&=Z_0^{i+1}\\ \omega_0^i+\omega_1^i+\omega_2^i&=\omega_0^{i+1}\\ \varphi_0^i+\varphi_1^i+\varphi_2^i&=\varphi_0^{i+1}\\ \kappa_0^i+\kappa_1^i+\kappa_2^i&=\kappa_0^{i+1} \end{aligned} \quad (11)$$

Similarly, imposing the first and second order continuity constraints for *X* function, we have:

$$\left.\frac{dX_C^i}{d\bar{t}}\right|_{\bar{t}=1}=\left.\frac{dX_C^{i+1}}{d\bar{t}}\right|_{\bar{t}=0} \quad (12)$$

and

$$\left.\frac{d^2X_C^i}{d\bar{t}^2}\right|_{\bar{t}=1}=\left.\frac{d^2X_C^{i+1}}{d\bar{t}^2}\right|_{\bar{t}=0} \quad (13)$$

In the same way, Equations 12 and 13 are written for the other external orientation functions, giving:

$$\begin{aligned} X_1^i+2X_2^i&=X_1^{i+1}\\ Y_1^i+2Y_2^i&=Y_1^{i+1}\\ Z_1^i+2Z_2^i&=Z_1^{i+1}\\ \omega_1^i+2\omega_2^i&=\omega_1^{i+1}\\ \varphi_1^i+2\varphi_2^i&=\varphi_1^{i+1}\\ \kappa_1^i+2\kappa_2^i&=\kappa_1^{i+1} \end{aligned} \quad (14)$$

for the first order derivative and:

$$\begin{aligned} X_2^i&=X_2^{i+1}\\ Y_2^i&=Y_2^{i+1}\\ Z_2^i&=Z_2^{i+1}\\ \omega_2^i&=\omega_2^{i+1}\\ \varphi_2^i&=\varphi_2^{i+1}\\ \kappa_2^i&=\kappa_2^{i+1} \end{aligned} \quad (15)$$

for the second order one.
Equations 10, 11, 14 and 15 are treated as soft (weighted) constraints.

3.2 Mathematical solution

The functions modelling the external orientation (Equation 7) are integrated into the collinearity equations (Equations 2 or 4), resulting in an indirect georeferencing model.
The collinearity equations are linearized with the first-order Taylor decomposition with respect to the unknown parameters modelling the sensor external orientation (x_{EO}), according to Equations 2 (or 4) and 7, and with respect to the unknown ground coordinates of the TPs (x_{TP}), according to Equation 7. As initial approximations, the parameters modelling the sensor external orientation (x_{EO}^0) are set equal to zero and the approximative ground coordinates of the TPs (x_{TP}^0) are estimated with forward intersection, using (X_{instr}, Y_{instr}, Z_{instr}, ω_{instr}, φ_{instr}, κ_{instr}) as external orientation.
Combining the observations equations and the constraints, the system:

$$\begin{cases} -e_{GCP}=A_{GCP}\,x_{EO} & -l_{GCP};P_{GCP}\\ -e_{TP}=A_{TP}\,x_{EO}+B_{TP}\,x_{TP} & -l_{TP};P_{TP}\\ -e_{C0}=C_0\,x_{EO} & -l_{C0};P_{C0}\\ -e_{C1}=C_1\,x_{EO} & -l_{C1};P_{C1}\\ -e_{C0}=C_2\,x_{EO} & -l_{C2};P_{C2} \end{cases} \quad (16)$$

is built, where:

x_{EO}: vector containing increments to x_{EO}^0;
x_{TP}: vector containing increments to;
A_{GCP}: design matrix for x_{EO} for GCPs observations;
A_{TP}: design matrix for x_{EO} for TPs observations;
B_{TP}: design matrix for x_{TP} for TPs observations;
C_0, C_1, C_2: design matrices for constraints on zero, first and second order continuity;
e: errors of measurements;
l: discrepancy vectors;
P: weight matrices for each group of observations.

GCPs and TPs are required in order to solve the system and estimate the unknown external orientation parameters and TPs ground coordinates.
Considering a sensor with *S* linear CCD arrays, N_{GCP} GCPs, N_{TP} TPs and n_s trajectory segments, the complete system contains $2xSx(N_{GCP+}N_{TP})$ collinearity equations, together with $6x(n_s-1)$ equations for each group of constraints described in Equations 10, 11, 14 and 15. The unknowns are $18xn_s$ for the external orientation and $3xN_{TP}$ for the TP ground coordinates.
The vectors x_{EO} and x_{TP} are estimated with least-squares adjustment and added to x_{EO}^0 and x_{TP}^0 in the next iteration. The process stops when x_{EO} and x_{TP} are smaller than suitable thresholds.

4. DATA SIMULATION

Simulated data were used in order to test the indirect georeferencing algorithm.
We assumed an airborne sensor, with the optical system consisting of one lens with focal length equal to 60.36 mm. The stereo viewing is achieved along-track with 3 linear CCD arrays scanning in forward (+21.2 deg), nadir and backward (-21.2 deg) directions (Figure 3).
Each linear CCD array consists of 10200 squared elements of dimension 7 μm.
Supposing 40832 exposures, the sensor position and attitude at each exposure (40832 x 6 data) were generated in a tangent local system with origin in the mean of the trajectory at null height, *X*- axis in East direction, *Y*- axis in North direction and *Z*- axis directed upwards. The aircraft was supposed to flight at a mean height of 500 m, along the trajectory shown in Figure 4, with a resulting ground pixel size of about 6cm.
40 GCPs were chosen in a 400 m large and 1600 m wide field, with the height in the range between 50 and 80 m. The distribution and height of the GCPs is shown in Figure 5. The resulting base over height ratio was about 0.7.

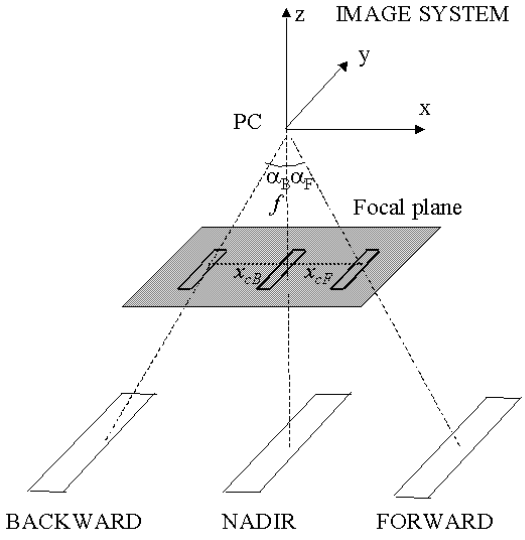

Figure 3. Geometry of simulated one-lens three-line sensors.

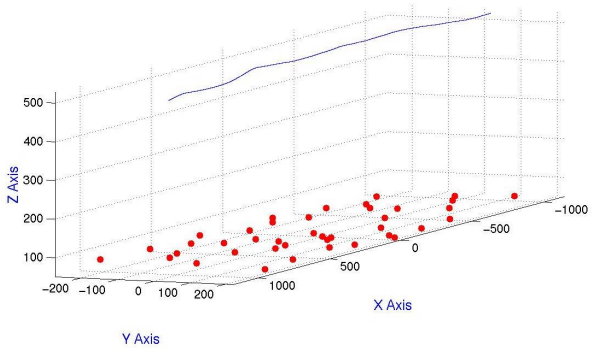

Figure 4. Simulated aircraft trajectory, together with GCPs.

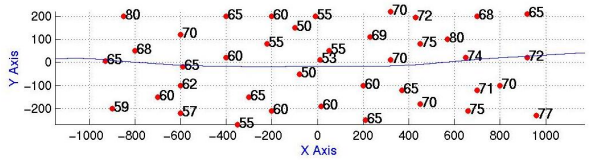

Figure 5. Distribution of simulated 40 GCPs, with their heights, in meters. The aircraft trajectory is also represented.

4.1 Back projection

The aim of back projection is to estimate the pixel coordinates (u= row number, v= column number) of the GCPs, using their known ground coordinates and the known external orientation for each sensor exposure.

The u coordinates can be determined from the well-known affine transformation between pixel and image coordinates:

$$y = \left(u - \frac{n_c}{2}\right) p_y \tag{17}$$

where n_c is the number of pixels per line and p_y the pixel size in y direction

Solving with respect to u and setting n_c=10200, it yields to:

$$u = 5100 + \frac{y}{p_y} \tag{18}$$

As far as v coordinate is concerned, it must be found at which time (or in correspondence of which image line) the ground point is observed by each CCD array. The first step is to calculate the image coordinates with Equation 2, using as external orientation the data corresponding to the first exposure. The computed image coordinates refer to a local system centred in the lens PC, with x-axis tangent to the flight trajectory, y-axis directed along the scanning direction and z-axis upwards directed. Then the calculated x- coordinate is compared to the theoretical one, called x_c, which is defined in the following way. According to the one-lens sensors geometry shown in Figure 3 and assuming that the linear CCD arrays are perpendicular to the flight direction and no distortions nor relative movements occur, x_c is constant for all CCD elements belonging to the same line (F=forward, N=nadir, B=backward) and is equal to:

$$\begin{aligned} x_{cF} &= f\ tan(\alpha_F) \\ x_{cN} &= f\ tan(\alpha_N) \\ x_{cB} &= f\ tan(\alpha_B) \end{aligned} \tag{19}$$

where $\alpha_{F,N,B}$ are the viewing angles and x_{cF}, x_{cN} and x_{cF} the theoretical x coordinates for the forward, nadir and backward viewing lines. As , α_N=0, x_{cN} results equal to 0.

If the difference between calculated and theoretical x-coordinates is bigger than the threshold of half the pixel size, the image coordinates are recomputed using the external orientation corresponding to the next exposure.

The procedure continues until the difference between calculated and theoretical x coordinates is smaller than the threshold. The corresponding exposure number will be then taken as v coordinate. The algorithm is applied to each GCPs for the forward, nadir and backward directions. As result, the GCPs image coordinates in the three images are obtained.

5. TEST ON SIMULATED DATA

In order to test the indirect georeferencing model, some perturbations in the known sensor external orientation (X_C, Y_C, Z_C, ω_C, φ_C, κ_C) were introduced and afterwards estimated using the indirect georeferencing algorithm. The perturbed position and attitude (X'_C, Y'_C, Z'_C, ω'_C, φ'_C, κ'_C) are defined for each exposure l (l = 1,…,Δl) as:

$$\begin{aligned} X'_C &= X_C + \Delta X + A_X \sin(n\cdot\pi\cdot l/\Delta l) \\ Y'_C &= Y_C + \Delta Y + A_Y \sin(n\cdot\pi\cdot l/\Delta l) \\ Z'_C &= Z_C + \Delta Z + A_Z \sin(n\cdot\pi\cdot l/\Delta l) \\ \omega'_C &= \omega_C + \Delta\omega + A_\omega \sin(n\cdot\pi\cdot l/\Delta l) \\ \varphi'_C &= \varphi_C + \Delta\varphi + A_\varphi \sin(n\cdot\pi\cdot l/\Delta l) \\ \kappa'_C &= \kappa_C + \Delta\kappa + A_\kappa \sin(n\cdot\pi\cdot l/\Delta l) \end{aligned} \tag{20}$$

where n is the number of cycles and Δl is the number of exposures. In the test, Δl= 40832, ΔX= ΔZ=2.0 m, ΔY=1.0 m, $\Delta\omega$=0.2°, $\Delta\varphi$= $\Delta\kappa$=0.3°, AX=AY=AZ=0.3m, $A\omega$= $A\varphi$= $A\kappa$=0.1° and n=5.

5.1 Results

The indirect georeferencing algorithm described in Equation 6 was tested in order to estimated the parameters modelling the sensor external orientation and the ground coordinates of the TPs. From the available 40 object points, a group of them was used as GCPs and the remaining as TPs. The TPs ground coordinates estimated by the triangulation were compared to their correct values and used for the tests' control. Various combinations of GCPs and TPs were chosen in order to evaluate the influence of the ground information. Table 1 provides a summary of the resulting absolute accuracy in the different test configurations. 6, 10 and 20 GCPs were tested, using 5 and 10 segments for the external orientation modelling. An absolute accuracy in the range 4-13 cm for *X*, 3-12 cm for *Y* and 8-19 cm for *Z* were achieved, corresponding to 0.6-2.1 pixels, 0.2-2 pixels and 1.3-3 pixels. Anyway the fact that the image coordinates were estimated at 0.5 pixels accuracy could have affected the results. The comparison between the results from the different tests confirms that the triangulation accuracy is influenced by the number and distribution of ground information and improves with the number of GCPs. As far as the modelling functions are concerned, the division of the trajectory in a larger number of segments does not imply any substantial improvements.

		GCPs+ TPs		
		20+20	10+30	6+34
5 segments	RMS_X	0.079	0.082	0.131
	RMS_Y	0.028	0.088	0.090
	RMS_Z	0.086	0.172	0.146
10 segments	RMS_X	0.041	0.050	0.057
	RMS_Y	0.059	0.099	0.124
	RMS_Z	0.112	0.138	0.192

Table 1. RMS values (in meters) of the estimated TPs coordinates.

6. CONCLUSIONS

A general sensor model for multi-line CCD array sensors with along stereo viewing has been presented. The model combines the classic photogrammetric collinearity equations with the sensor external orientation modelling, resulting in an integrated triangulation. The functions used to describe the external orientation are based on piecewise polynomials. The model can be applied on sensors carried on both airplane and satellites, with optical systems consisting of one or more lenses. The algorithm can also include and correct any external orientation observations provided by GPS and INS instruments carried on board.

The proposed model has been tested on a simulated sensor (1 lens, 3 CCD arrays) carried on airplane, with different GCPs and TPs distributions. The results have been presented. An accuracy in the range of 0.6-2.1 pixels in *X*, 0.2-2 pixels in *Y* and 1.3-3 pixels in *Z* was achieved using 6, 10 and 20 GCPs and dividing the trajectory in 5 and 10 segments.

In the next future, the model will be applied to a real dataset from the Japanese TLS (Three-Line Sensor), by Starlabo, Tokyo.

7. ACKNOWLEDGMENTS

This work is part of Cloudmap2 project, funded by the European Commission under the Fifth Framework program for Energy, Environment and Sustainable Development.

I would like to thank Mr. Zhang Li, from my department, for his helpful suggestions.

8. REFERENCES

Chen, T., 2001. High precision georeference for airborne Three-Line Scanner (TLS) imagery. Proceedings of 3rd International Image Sensing Seminar on New Development in Digital Photogrammetry, Gifu, Japan, pp. 71-82.

Cramer, M., Stallmann, D., Haala, N., 2000. Direct georeferencing using GPS/INS exterior orientations for photogrammetric applications. International Archives of Photogrammetry and Remote Sensing, Vol. 33, Part B3, Amsterdam, pp. 198-205.

Ebner, H., Kornus, W., Ohlhof, T., 1992. A simulation study on point determination for the MOMS-027D2 space project using an extended functional model. International Archives of Photogrammetry and Remote Sensing, Vol. 29, Part B4, Washington D.C., pp. 458-464.

Haala, N., Stallmann, D., Cramer, M., 1998. Calibration of directly measured position and attitude by aerotriangulation of three-line airborne imagery. Proceedings of ISPRS Commission III Symposium on Object Recognition and Scene Classifications from Multispectral and Multisensor Pixels, Ohio, Columbus, pp. 28-30.

Kratky, V., 1989. Rigorous photogrammetric processing of SPOT images at CCM Canada. ISPRS Journal of Photogrammetry and Remote Sensing, No. 44, pp. 53-71.

Lee, C., Theiss, H.J., Bethel, J.S., Mikhail, E.M., 2000. Rigorous mathematical modeling of airborne pushbroom imaging systems. Photogrammetric Engineering & Remote Sensing, Vol. 66, No. 4, pp. 385-392.

Poli, D., 2001. Direct georeferencing of multi-line images with a general sensor model. ISPRS Workshop "High resolution mapping from space 2001", 18-21 September 2001, Hanover. Proceedings on CD.

Schwarz, K.P., 1996. Aircraft position and attitude determinations by GPS and INS. International Archives of Photogrammetry and Remote Sensing, Vol. 31, Part B2, Vienna, pp. 67-73.

Tempelmann, U., Boerner, A., Chaplin, B., Hinsken, L., Mykhalevych, B., Miller, S., Recke, U., Reulke, R., Uebbing, R., 2000. Photogrammetric software for the LH systems ADS40. International Archives of Photogrammetry and Remote Sensing, Vol. 33, Part B2, Amsterdam, pp. 552-559.